Hindawi
Mathematical Problems in Engineering
Volume 2018, Article ID 2372305, 18 pages
https://doi.org/10.1155/2018/2372305

Research Article

Quadratic Integral Sliding Mode Control for Nonlinear Harmonic Gear Drive Systems with Mismatched Uncertainties

Runze Ding and Lingfei Xiao

College of Energy and Power Engineering, Nanjing University of Aeronautics and Astronautics, Nanjing, China

Correspondence should be addressed to Lingfei Xiao; lfxiao@nuaa.edu.cn

Received 8 December 2017; Revised 1 May 2018; Accepted 3 June 2018; Published 22 July 2018

Academic Editor: Javier Martinez Torres

For a class of nonlinear harmonic gear drive systems with mismatched uncertainties, a novel robust control method is presented on the basis of quadratic integral sliding mode surface, and the closed-loop system has satisfying performance and strong robustness against mismatched uncertainties and nonlinear disturbances. Considering time-varying nonlinear torques and parameters variations which are caused by nonlinear frictions and backlash, a nonlinear harmonic gear drive system mathematic model is established and the effect of nonlinear parts is compensated during control system design. It is proven that the quadratic integral sliding mode surface can be reached in finite time and the closed-loop system is asymptotic stable robustly. The simulation studies are carried out in comparison with traditional linear sliding mode control and integral sliding mode control, verifying the effectiveness of the proposed method.

1. Introduction

Harmonic gear is a new type of drive which is realized by elastic deformation movement. Instead of using rigid component, it uses a flexible component to realize the drive. Therefore, it has many special properties which cannot be obtained in other drives. The harmonic gear is composed of three main components, including a circular spline, a flexspline, and a wave generator. Through the action of the wave generator, a movable deformation wave is generated in the flexspline and the flexspline engages with the circular spline to achieve the transmission. The harmonic gear has advantages of large range of transmission ratio, multiteeth gearing, large carrying capacity, high precision, and running smoothly without impact. Because of its own characteristics, harmonic gear is widely applied in aviation control systems, instrumentation, robotics, and other fields [1–4], where drive systems are required to be capable of small volume, light weight, high transmission precision, and small hysteresis.

Despite those advantages, many issues will occur during runtime, such as assembly errors, gear wears, and deterioration of working environment. Due to kinetic errors and nonlinear elastic deformations, these issues will cause motion delay, transmission errors, and inaccurate tracking, which leads to the fact that it is very important to focus on angular transmission errors in harmonic gear drive systems.

In order to reduce the errors, many researchers have done wide investigations on force analysis and movement analysis. The stress of flexspline in harmonic gear drive is analyzed in [5]. At same time, a harmonic gear drive system dynamic system is established by dynamic equation analysis and least square method in [6]. In [7], the research of theoretical modeling of nonlinear torsional behavior in harmonic gear is carried out. These researches abovementioned focus on harmonic gear drive systems' dynamic model, analysis of errors in harmonic gear drive systems, or nonlinear frictions model, which illustrates the fact that angular transmission errors of harmonic gear drive system have been widely analyzed and have been mathematically modeled in various conventional studies and make it practical to compensate the error by control methods.

However, there are fewer researches on this part and one primary reason for this is harmonic gear drive system, a class of nonlinear systems, which are affected by mismatched uncertainties such as nonlinear torques and working condition deterioration. It is hard to control such nonlinear systems with mismatched uncertainties and nonlinear disturbances. Consequently, researches in this area are developed

slowly. Previous research [8] designs a PID controller for a class of harmonic drive system with frictions to reduce transmission errors, and as a result, harmonic gear drive system's performance is enhanced by error compensation. The results show that using control method to reduce error is feasible but [8] failed to consider mismatched uncertainties and nonlinear disturbances, which are inevitable in practice, while [9] designing a sliding mode controller based on linear sliding mode surface, which has a better performance than PID controller, and taking disturbances into consideration. Though it has its improvements, there are also some limitations in [9] such as ignoring some critical torques in modeling and designing, using linear sliding mode surface and no attention to uncertainties.

Sliding mode control (SMC) is a new variable structure robust control method. By choosing the sliding surface and the reaching law, it can make the system response quickly with strong robustness and have insensibility to external interferences and parameters variations. As an important method of nonlinear control, it has been widely researched in recent years.

In [10], Xie Jian et al. design a sliding mode controller for hydraulic pump-control-motor system and use simulation results to illustrate that the sliding mode controller has strong anti-interference ability and good tracking performance when compared with PID controller, improving the control accuracy and stability of the system. In [11], by using boundary layer method to restrain the chatting, NE Sadr et al. design a sliding mode controller for missile autopilot and the system has strong robustness to uncertainties and disturbances. Besides, Murat Furat et al. design a second-order integral sliding mode controller for a SISO system in [12], making the system overcome the parameter fluctuation and uncertainties caused by the external load. Furthermore, Azar A T et al. design an adaptive sliding mode controller for the Furuta Pendulum in [13]. In comparison with other controllers, the simulation result shows that the sliding mode control has advantages of fast response and small errors. In addition, Ginoya D et al. design a sliding mode controller using extended disturbance observer for a system with uncertainties in [14] and the closed-loop system has robustness to the uncertainties. Hess RA et al. design a slide mode controller for a nonlinear unmanned aerial vehicle in [15], and the controller has a good performance on nonlinear system.

Investigations in [10–15] illustrate that the sliding mode control method finds widel applications on nonlinear system control and has a good performance. Besides, the closed-loop system has insensitivity to disturbance and uncertainties, which means that the system has strong robustness against uncertainties including parameters variations and disturbances. However, the insensitivity to uncertainties is realized only in sliding phase. If system is not on the sliding mode surface, the system will be vulnerable to uncertainties. Additionally, the robustness is only limited to matched uncertainties. The so-called integral sliding mode control (ISMC) is proposed to improve such situation but, unfortunately, the performance of ISMC is conservative.

A class of nonlinear harmonic gear drive systems with mismatched uncertainties is studied and the primary contributions of this paper are as follows. (1) A novel quadratic integral sliding mode controller design method is presented on the basis of quadratic integral sliding mode surface. (2) Considering frictions, time-varying nonlinear torques, and parameters variations which are caused by backlash, the influence of nonlinear parts on control system has been studied. The mathematical models of nonlinear torques and frictions are presented and the effect of nonlinear parts is compensated during control system design. (3) In system modeling, take frictions and nonlinear elastic deformation into consideration and the mathematical model of harmonic gear drive system is established. (4) By using Lyapunov stability theory, it is proven that the quadratic integral sliding mode surface can be reached in finite time and the closed-loop system is robustly asymptotic stable. (5) In comparison with the traditional linear sliding mode control (which can be abbreviated as SMC) and the integral sliding mode control (which can be abbreviated as ISMC), the simulation results demonstrated that quadratic integral sliding mode control (which can be abbreviated as QISMC) stabilizes the system rapidly with fast response, short rise time, small overshoot, small error, and strong robustness against the mismatched uncertainties and nonlinear disturbances.

The remainder of this paper is organized as follows. Section 2 gives details on harmonic gear drive systems modeling and illustrations for backlash and frictions. In Section 3, the quadratic integral sliding surface is presented; furthermore, its corresponding quadratic integral sliding mode controller is designed in Section 4. Section 5 proves that quadratic integral sliding mode surface can be reached in finite time and the closed-loop system is robustly asymptotic stable. The effectiveness of the quadratic integral sliding mode control is verified in comparison with SMC and ISMC in Section 6, and Section 7 draws the conclusions of this paper.

2. Harmonic Gear Drive System

Harmonic gear drive system (Figure 1) is mainly divided into the DC motor system and the harmonic gear system. The DC motor is driven by controller and outputs torques to the wave generator in harmonic gear system; as a result, torques are transmitted by engagement to a flexspline. A mathematical description of harmonic gear drive system will be given in this part.

2.1. DC Motor System. Using Kirchhoff's law of electricity, DC motor system can be presented by the following:

$$u(t) = i_a R + L\frac{di_a}{dt} + K_b\omega_m \tag{1}$$

where i_a is the motor armature current, $u(t)$ is the motor armature voltage, R is the equivalent resistance, K_b is the back-EMF coefficient, and ω_m is the angel speed of motor rotor. L is the motor armature inductance, which is generally ignored due to its tiny value.

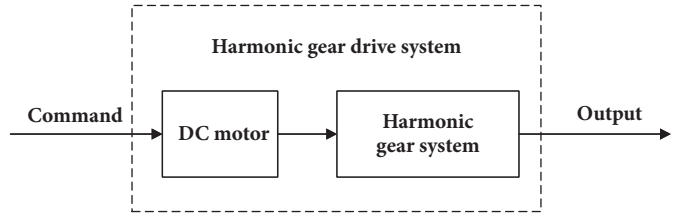

Figure 1: Structure of Harmonic gear drive system.

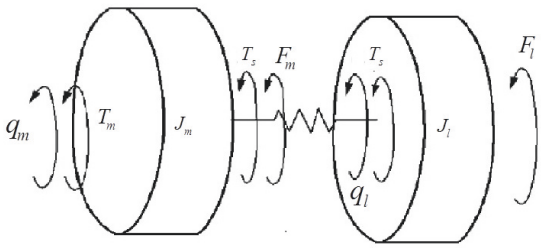

Figure 2: Harmonic gear system.

2.2. Harmonic Gear System. As Figure 2 [16] shows, harmonic gear system can be simplified as a typical two-mass system including a circular spline, a flexspline, and a wave generator.

Harmonic gear transmission system satisfies following dynamic equations:

$$\begin{aligned} J_m\ddot{q}_m &= T_m - T_s - F_m \\ J_l\ddot{q}_l &= T_s - F_l \end{aligned} \tag{2}$$

where q_m is the angular displacement of the wave generator, q_l is the angular displacement of the flexspline, T_m is the torques on the wave generator, and T_s is the torques on the flexspline. F_m is the equivalent frictions on the wave generator and F_l is the equivalent frictions on the flexspline. J_m is the moment of inertia of the wave generator and J_l is the moment of inertia of the flexspline.

The kinetic model of harmonic gear drive system satisfies the following:

$$T_s = K_s\left(\frac{q_m}{r} - q_l\right) \tag{3}$$

$$T_m = K_m i_a \tag{4}$$

where r is the reduction ratio, K_s is the torsional stiffness of the harmonic gear, and K_m is the motor torque coefficient.

(1) gives

$$i_a = \frac{-K_b\dot{q}_m + u(t)}{R} \tag{5}$$

Substituting i_a into (4), it would be followed that

$$T_m = -\frac{K_m K_b}{R}\dot{q}_m + \frac{K_m}{R}u(t) \tag{6}$$

Substituting (3) and (6) into (2), one can obtain harmonic gear drive systems kinetic model:

$$\begin{aligned} J_m\ddot{q}_m &= \frac{K_m}{R}u(t) - K_s\left(\frac{q_m}{r} - q_l\right) - \frac{K_m K_b}{R}\dot{q}_m + F_m \\ J_l\ddot{q}_l &= K_s\left(\frac{q_m}{r} - q_l\right) - F_l \end{aligned} \tag{7}$$

Considering the frictions model [16], because the angle range in accurate control is small, it is acceptable to choose the average Coulomb's frictions f_{cm} as whole frictions in harmonic gear drive systems.

$$f_{cm} = s_1 q_m^2 + s_2 q_m + s_3 \tag{8}$$

The static frictions f_{sm} is about 3.88% larger than f_{cm}; then one can obtain

$$f_{sm} = 1.0388 \times f_{cm} \tag{9}$$

And frictions on wave generator $F_m(x)$ is

$$F_m(x) = \begin{cases} -\psi_m, & \dot{q}_m = 0,\ |\psi_m| \le f_{sm} \\ -\mathrm{sgn}(\psi_m) f_{sm}, & \dot{q}_m = 0,\ |\psi_m| > f_{sm} \\ -\mathrm{sgn}(q_m) f_{cm}, & |\dot{q}_m| > 0 \end{cases} \tag{10}$$

where $\psi_m = -K_s(q_m/r - q_l) + (K_m/R)u(t)$.

In the same way, frictions on the flexspline $F_l(x)$ would be as follows:

$$F_l(x) = \begin{cases} -\psi_l, & \dot{q}_l = 0,\ |\psi_l| \le f_{sl} \\ -\mathrm{sgn}(\psi_l) f_{sl}, & \dot{q}_l = 0,\ |\psi_l| > f_{sl} \\ -\mathrm{sgn}(q_l) f_{cl}, & |\dot{q}_l| > 0 \end{cases} \tag{11}$$

where $\psi_l = (1/r)K_s(q_m/r - q_l)$.

The gears will heat because of frictions in gear drive system. Correspondingly, a gap which is called backlash [17] is designed as the expansion space for gears (shown in Figure 3). These gaps will continue to increase due to wears

and frictions caused by repeated stop, variable speed, the working environment, and other reasons, finally leading to motion delay and inaccurate tracking.

A mathematical expression of backlash is introduced in [18], considering the dead-zone model, and defines the elastic deformation torsion angle $\Delta e(t)$ caused by backlash as

$$\Delta e(t) = \begin{cases} -\Delta\varphi - j, & \dfrac{q_m(t)}{r} - q_l(t) - \Delta\varphi > j \\ 0, & \left|\dfrac{q_m(t)}{r} - q_l(t) - \Delta\varphi\right| < j \\ -\Delta\varphi + j, & \dfrac{q_m(t)}{r} - q_l(t) - \Delta\varphi < -j \end{cases} \tag{12}$$

where j is the width of backlash and $\Delta\varphi$ is the transmission error caused by nonelastic deformation torsion angle, which can be approximated by random number model. The $\Delta e(t)$ dead-zone model can be presented by Figure 4.

Because of $\Delta e(t)$, a nonlinear torque $T_{ul}(x) = K_s \Delta e(t)$ is attached to harmonic gear drive systems. In addition, it is inevitable that system parameters and characteristics will drift slowly due to factors such as gear wear and environment. As a result, choose ΔAx as the state parameters variations and ΔB as the control signals variations.

Choose state vectors as $[x_1 \ x_2 \ x_3 \ x_4]^T = [q_m \ \dot{q}_m \ q_l \ \dot{q}_l]^T$ and harmonic gear drive systems can be presented as follows:

$$\begin{cases} \dot{x}_1 = x_2 \\ \dot{x}_2 = -\varphi_{21}x_1 - \varphi_{22}x_2 + \varphi_{23}x_3 - T_{ul}(x) + T_m(x) + \varphi_{2u}u(t) \\ \dot{x}_3 = x_4 \\ \dot{x}_4 = \varphi_{41}x_1 - \varphi_{43}x_3 + T_{ul}(x) + T_l(x) \end{cases} + \Delta Ax + \Delta Bu(t) \tag{13}$$

$$\begin{aligned} \varphi_{21} &= \frac{K_s}{rJ_m}, \\ \varphi_{22} &= \frac{K_m K_b}{J_m R}, \\ \varphi_{23} &= \frac{K_s}{J_m}, \\ T_m(x) &= \frac{F_m(x)}{J_m} \\ \varphi_{2u} &= \frac{K_m}{J_m R}, \\ \varphi_{41} &= \frac{K_s}{rJ_l}, \\ \varphi_{43} &= \frac{K_s}{J_l}, \\ T_l(x) &= \frac{F_l(x)}{J_l} \end{aligned} \tag{14}$$

It is shown in (13) and (14) that the system of harmonic gear drive system is a class of nonlinear system with mismatched uncertainties including parameters perturbation and external disturbance.

3. Quadratic Integral Sliding Mode Design

In this part, a quadratic integral sliding mode surface is designed to compensate the influence of mismatched uncertainties and a detailed analysis of system in sliding mode is given to verify the effectiveness of proposed method.

Consider an arbitrary nonlinear system with mismatched uncertainties as follows:

$$\dot{x} = f(x,t) + \Delta f(x,t) + [g(x,t) + \Delta g(x,t)]u \tag{15}$$

where $x \in R^n$ is state vector, $u \in R$ is control signal, and $f(x,t) = [f_1(x,t) \ f_2(x,t) \ \dots \ f_4(x,t)]^T$ are nonlinear

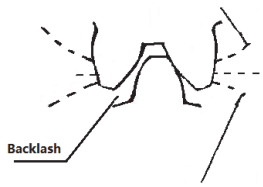

Figure 3: Backlash.

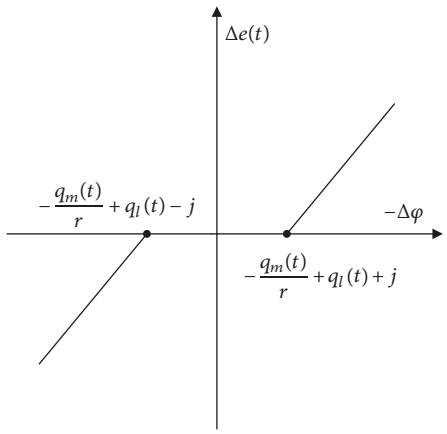

Figure 4: $\Delta e(t)$ dead-zone model.

dynamic vectors. $g(x,t) = [g_1(x,t)\ \ g_2(x,t)\ \ \dots\ \ g_4(x,t)]^T$ are nonlinear control gain vectors, $\Delta f(x,t) = [\Delta f_1(x,t)\ \ \Delta f_2(x,t)\ \ \dots\ \ \Delta f_4(x,t)]^T$ are parameters perturbations and external disturbances, and $\Delta g(x,t) = [\Delta g_1(x,t)\ \ \Delta g_2(x,t)\ \ \dots\ \ \Delta g_4(x,t)]^T$ are parameters perturbations of control gain. Here, $\Delta f(x,t) + \Delta g(x,t)u$ are uncertainties.

Suppose that there exists a control law u_0, which is designed in a desired way, stabilizing nominal system (16), with a given accuracy (the nominal system is the system without uncertainties).

$$\dot{\overline{x}} = f(x,t) + g(x,t)\,u_0 \tag{16}$$

Considering the nonlinear system with mismatched uncertainties (15), the uncertainties are unknown, but it is acceptable to assume that the uncertainties are bounded. Consequently, assumptions are introduced as follows.

Assumption 1. $\|\Delta f(x,t)\| \le \xi_1\|x\| + \xi_0 \le \|f(x,t)\|$, with the scalars $\xi_0 > 0,\ \xi_1 > 0$; here$\|\cdot\|$ stands for Euclidean norm.

Assumption 2. $\|\Delta g(x,t)\| \le \zeta_1\|x\| + \zeta_0 \le \|g(x,t)\|$, with the scalars $\zeta_0 > 0,\ \zeta_1 > 0$; here$\|\cdot\|$ stands for Euclidean norm.

The quadratic integral sliding mode control law will be designed as

$$u = u_0 + u_1 \tag{17}$$

where u_0 stands for the abovementioned control law of nominal system, which is responsible for the performance of the nominal system and satisfies **Assumption 3**.

Assumption 3. $u_0 \le \beta_0 + \beta_1\|x\|$, with the scalars $\beta_0 > 0,\ \beta_1 > 0$.

While u_1 stands for discontinuous control action that compensates the mismatched uncertainties, based on quadratic integral sliding mode surface, the definition of u_1 will be introduced in (32).

In order to compensate the effect of mismatched uncertainties, the quadratic integral sliding mode surface is designed as

$$\begin{aligned} s = {} & \frac{1}{2}\left[x^T(t)\,x(t) - x(t_0)^T\,x(t_0)\right] \\ & - \int_{t_0}^{t}\left\{x^T(t)\left[f(x,t) + g(x,t)\,u\right] - b(x)\,u_1\right\}dt \end{aligned} \tag{18}$$

Here $x(t_0)$ is the initial values of the state vector and $b(x) \in R$ is demonstrated in (19)

$$b(x) = \sigma + \zeta_0\|x\| + \zeta_1\|x\|^2 + \left\|x^T(t)\,g(x,t)\right\| \tag{19}$$

with the arbitrary scalar $\sigma > 0$.

The sliding mode surface (18) is in a quadratic form; therefore, (18) is a quadratic integral sliding mode surface. Assuming that the quadratic integral sliding mode surface $s = 0$ can be reached, it leads to

$$\begin{aligned} & \frac{1}{2}\left[x^T(t)\,x(t) - x(t_0)^T\,x(t_0)\right] \\ & \quad - \int_{t_0}^{t}\left\{x^T(t)\left[f(x,t) + g(x,t)\,u\right] - b(x)\,u_1\right\}dt \\ & = 0 \end{aligned} \tag{20}$$

and the following can be obtained:

$$\begin{aligned} s = {} & \int_{t_0}^{t}\left\{x^T(t)\left[\Delta f(x,t) + \Delta g(x,t)\,u\right] + b(x)\,u_1\right\}dt \\ & = 0 \end{aligned} \tag{21}$$

If the quadratic integral sliding mode surface (21) is reached and remains there, then

$$\dot{s} = x^T(t)\left[\Delta f(x,t) + \Delta g(x,t)\,u\right] + b(x)\,u_1 = 0 \tag{22}$$

One can obtain the equivalent control of u_1:

$$u_{1eq} = -\frac{x^T(t)\left[\Delta f(x,t) + \Delta g(x,t)\,u_0\right]}{\left[x(t)^T\Delta g(x,t) + b(x)\right]} \tag{23}$$

Substituting u_{1eq} into (15), then the system in sliding mode will be

$$\begin{aligned} \dot{x} = {} & f(x,t) + g(x,t)\,u_0 + \triangle f(x,t)\,I_n\Gamma \\ & + \triangle g(x,t)\,u_0 I_n\Gamma \end{aligned} \tag{24}$$

where $\Gamma = 1 - x^T(t)[g(x,t) + \triangle g(x,t)]/(x^T\triangle g(x,t) + b(x))$ and Γ could be written into

$$\Gamma = 1 - \left[\frac{x^T(t)\,g(x,t) + x^T(t)\,\triangle\, g(x,t)}{x^T(t)\,\triangle\, g(x,t) + b(x)}\right] \tag{25}$$

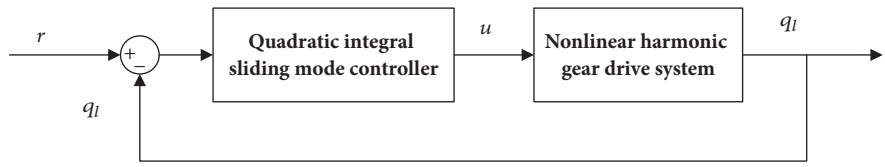

Figure 5: Structure of control system for harmonic gear drive systems.

It is evident that

$$\Gamma = \frac{b(x) - x^T(t)\, g(x,t)}{b(x) + x^T(t) \triangle g(x,t)} \tag{26}$$

Consider that

$$\begin{aligned} -\left\|x^T(t)\, g(x,t)\right\| &\le -x^T(t)\, g(x,t) \le \left\|x^T(t)\, g(x,t)\right\| \\ -\zeta_1 \|x\|^2 - \zeta_0 \|x\| &\le x^T(t) \triangle g(x,t) \\ &\le \zeta_1 \|x\|^2 + \zeta_0 \|x\| \end{aligned} \tag{27}$$

Taking **Assumption 2** and (19) into consideration, it would follow that

$$\begin{aligned} b(x) - x^T(t)\, g(x,t) &\le \sigma + \zeta_1 \|x\|^2 + \zeta_0 \|x\| \\ \sigma + \left\|x^T(t)\, g(x,t)\right\| &\le x^T(t) \triangle g(x,t) + b(x) \end{aligned} \tag{28}$$

Then

$$\Gamma \le \frac{\sigma + \zeta_1 \|x\|^2 + \zeta_0 \|x\|}{\sigma + \left\|x^T(t)\, g(x,t)\right\|} \le 1 \tag{29}$$

Besides

$$\begin{aligned} 0 < \sigma &\le b(x) - x^T(t)\, g(x,t) \\ 0 < \sigma &\le b(x) - x^T(t) \triangle g(x,t) \end{aligned} \tag{30}$$

One can obtain the conclusion

$$0 < \Gamma \le 1 \tag{31}$$

It is obvious that the effect of uncertainties is compensated. Equation (31) indicates that if the quadratic integral sliding mode surface is reached and remains there, the effect of uncertainties $\Delta f(x,t) + \Delta g(x,t)u_0$ can be compensated, achieving robustness to mismatched uncertainties. Besides, the system will be on sliding mode surface from any initial state; consequently, the system is robust to mismatched uncertainties from any initial state.

4. Quadratic Integral Sliding Mode Controller Design

The design of the abovementioned quadratic integral sliding mode controller will be illustrated in this part. The structure of the quadratic integral sliding mode controller is shown in Figure 5.

As was mentioned earlier, the quadratic integral sliding mode control law will be designed as $u = u_0 + u_1$. Then u_1 is the discontinuous control action that compensates the mismatched uncertainties, with definition as

$$\begin{aligned} &u_1 \\ &\quad = -b^{-1}(x)\left[\left(\lambda_0 + \lambda_1 \|x\|\right) s + \left(\eta_0 + \eta_1 \|x\|\right) \operatorname{sgn}(s)\right] \end{aligned} \tag{32}$$

where λ_0, λ_1, η_0, and $\eta_1 \in R$ are scalars defined as follows:

$$\lambda_0 \ge \frac{\varepsilon_1 \left(\zeta_1 \|x\|^2 + \zeta_0 \|x\| + \sigma\right)}{\sigma} \tag{33}$$

$$\lambda_1 \ge 0 \tag{34}$$

$$\eta_0 \ge \frac{\varepsilon_2 \left(\zeta_1 \|x\|^2 + \zeta_0 \|x\| + \sigma\right)}{\sigma} \tag{35}$$

$$\begin{aligned} \eta_1 &\ge (\sigma\delta)^{-1} \\ &\quad \cdot \left[\xi_0 + \zeta_0\beta_0 + \left(\xi_1 + \zeta_0\beta_1 + \zeta_1\beta_0\right)\|x\| + \zeta_1\beta_1 \|x\|^2\right] \end{aligned} \tag{36}$$

The two approaching parameters ε_1 and ε_2 in (33) and (35) are arbitrary positive scalars, and $\delta = (\sigma + \zeta_0\|x\| + \zeta_1\|x\|^2)^{-1}$.

The sliding mode control will inevitably cause chattering due to switching time lag, spatial lag, and inertia effect. Chattering will affect the control precision and reduce systems control quality, in more serious cases, and even destroy control elements. In most investigations, the sign function is replaced with the saturation function to reduce the chattering. To some degree, this method can weaken the chattering, but the saturation function is a discontinuous function, making the result conservative. In this paper, the sign function is replaced by the hyperbolic tangent function, which is continuous and smooth.

Hyperbolic tangent function is shown as follows:

$$\tanh\left(\frac{s}{\varepsilon}\right) = \frac{e^{s/\varepsilon} - e^{-s/\varepsilon}}{e^{s/\varepsilon} + e^{-s/\varepsilon}} \tag{37}$$

where s stands for the quadratic integral sliding mode and $\varepsilon > 0$ is a positive scalar, which decides the change rate of hyperbolic tangent inflection point.

5. Harmonic Gear Drive Systems Stability

The reachability of the sliding mode surface and the stability of closed-loop system under quadratic sliding mode control will be proved in this part.

Reachability of the Sliding Mode. Derivation of the quadratic integral sliding mode surface (18) along time and substituting (15) into (18), differential of (18) would be

$$\dot{s} = x^T(t)\left[\Delta f(x,t) + \Delta g(x,t)u\right] + b(x)u_1 \tag{38}$$

By using the quadratic sliding mode control law (33)-(36), the following equations can be obtained:

$$\begin{aligned} s\dot{s} &= x^T(t)\Delta f(x,t)s + sx^T(t)\Delta g(x,t)u + sb(x) \\ &\cdot \left\{-b^{-1}(x)\left[\left(\lambda_0 + \lambda_1\|x\|\right)s + \left(\eta_0 + \eta_1\|x\|\right)\operatorname{sgn}(s)\right]\right\} \\ &= x^T(t)\Delta f(x,t)s + sx^T(t)\Delta g(x,t)u - \left(\lambda_0\right. \\ &\left. + \lambda_1\|x\|\right)s^2 - \left(\eta_0 + \eta_1\|x\|\right)|s| \end{aligned} \tag{39}$$

where

$$\begin{aligned} sx^T(t)\Delta g(x,t)u &= sx^T(t)\Delta g(x,t)\left\{u_0\right. \\ &\left. - b^{-1}(x)\left[\left(\lambda_0 + \lambda_1\|x\|\right)s + \left(\eta_0 + \eta_1\|x\|\right)\operatorname{sgn}(s)\right]\right\} \\ &= sx^T(t)\Delta g(x,t)u_0 - x^T(t)\Delta g(x,t)b^{-1}(x) \\ &\cdot \left(\left(\lambda_0 + \lambda_1\|x\|\right)s^2 + \left(\eta_0 + \eta_1\|x\|\right)|s|\right) \end{aligned} \tag{40}$$

and then

$$\begin{aligned} s\dot{s} &= x^T(t)\Delta f(x,t)s + sx^T(t)\Delta g(x,t)u_0 - x^T(t) \\ &\cdot \Delta g(x,t)b^{-1}(x) \\ &\cdot \left(\left(\lambda_0 + \lambda_1\|x\|\right)s^2 + \left(\eta_0 + \eta_1\|x\|\right)|s|\right) \\ &- \left(\left(\lambda_0 + \lambda_1\|x\|\right)s^2 + \left(\eta_0 + \eta_1\|x\|\right)|s|\right) = x^T(t) \\ &\cdot \Delta f(x,t)s + sx^T(t)\Delta g(x,t)u_0 \\ &- \left(1 + x^T(t)\Delta g(x,t)b^{-1}(x)\right) \\ &\cdot \left[\left(\lambda_0 + \lambda_1\|x\|\right)s^2 + \left(\eta_0 + \eta_1\|x\|\right)|s|\right] \end{aligned} \tag{41}$$

Because of **Assumption 1**, **Assumption 2,** and **Assumption 3**, the inequation above will be

$$\begin{aligned} s\dot{s} &\le \left[\left(\xi_1\|x\| + \xi_0\right) + \left(\zeta_1\|x\| + \zeta_0\right)\left(\beta_0 + \beta_1\|x\|\right)\right]\|x\| \\ &\cdot |s| + \left[x^T(t)\Delta g(x,t)b^{-1}(x)\right] \\ &\cdot \left[\left(\lambda_0 + \lambda_1\|x\|\right)s^2 + \left(\eta_0 + \eta_1\|x\|\right)|s|\right] \\ &- \left[\left(\lambda_0 + \lambda_1\|x\|\right)s^2 + \left(\eta_0 + \eta_1\|x\|\right)|s|\right] \\ &\le \left[\left(\xi_1\|x\| + \xi_0\right) + \left(\zeta_1\|x\| + \zeta_0\right)\left(\beta_0 + \beta_1\|x\|\right)\right]\|x\| \\ &\cdot |s| + \left[\|x\|\left(\zeta_1\|x\| + \zeta_0\right)b^{-1}(x) - 1\right] \\ &\cdot \left[\left(\lambda_0 + \lambda_1\|x\|\right)s^2 + \left(\eta_0 + \eta_1\|x\|\right)|s|\right] \end{aligned} \tag{42}$$

Considering (19), it would lead to

$$\begin{aligned} s\dot{s} &\le \left\{\xi_0 + \zeta_0\beta_0 + \left(\xi_1 + \zeta_0\beta_1 + \zeta_1\beta_0\right)\|x\| + \zeta_1\beta_1\|x\|^2\right\} \\ &\cdot \|x\| \cdot |s| - \frac{\sigma + \left\|x^T(t)g(x)\right\|}{b(x)}\left(\lambda_0 + \lambda_1\|x\|\right)s^2 \\ &- \frac{\sigma + \left\|x^T(t)g(x)\right\|}{b(x)}\left(\eta_0 + \eta_1\|x\|\right)|s| \end{aligned} \tag{43}$$

Considering (33) to (36), then $s\dot{s} \le -\varepsilon_1 s^2 - \varepsilon_2|s|$.

In consequence, the quadratic integral sliding mode surface (18) can be reached in finite time and remains there.

This completes the proof. □

Stability of the Closed-Loop System in Sliding Mode. Select the Lyapunov function as

$$V(x) = \frac{1}{2}x^T(t)x(t) \tag{44}$$

$$\begin{aligned} \dot{V}(x) &= x^T(t)\dot{x}(t) = x^T(t) \\ &\cdot \left[f(x,t) + \Delta f(x,t) + g(x,t)u + \Delta g(x,t)u\right] \end{aligned} \tag{45}$$

The quadratic integral sliding mode surface (18) has been proved to be reachable. If the system reaches the surface and remains there, then

$$x^T(t)\left[\Delta f(x,t) + \Delta g(x,t)u\right] + b(x)u_1 = 0 \tag{46}$$

Substituting (46) into (45), one can obtain

$$\dot{V}(x) = x^T(t)\left[f(x,t) + g(x,t)u_0 + b(x)u_1\right] \tag{47}$$

When (18) is reached, then $u_1 = 0$ and (47) will be

$$\dot{V}(x) = x^T(t)\left[f(x,t) + g(x,t)u_0\right] \tag{48}$$

It can be seen that if the nominal system (16) can be stabilized by u_0, then $\dot{V}(x) < 0$. In other words, if u_0 is designed to stabilized the nominal system (16), then the closed-loop nonlinear system with mismatched system is asymptotically stable under the quadratic integral sliding mode control law u.

This completes the proof. □

In conclusion, it is proved that the quadratic sliding mode surface (18) is reachable and the closed-loop nonlinear system with mismatched uncertainties in sliding mode is asymptotically stable with robustness to mismatched uncertainties. The system's dynamic performance is depended on u_0, and various control theories (such as LQR, H-infinity control) could be applied in u_0 designing according to different requirements.

Table 1: Simulation parameters.

Parameter	Unit	Value
R	Ω	5.6
K_m	$N \cdot m \cdot A^{-1}$	0.517
K_e	$V \cdot s \cdot rad^{-1}$	0.517
J_m	$Kg \cdot m^2$	6.82×10^{-4}
J_l	$Kg \cdot m^2$	2.35×10^{-2}
r		80
K_s	$Nm \cdot rad^{-1}$	$5.4 \times 10^5 \left(\left\|T_s\right\| < 235Nm\right)$ $8.8 \times 10^5 (235Nm \le \left\|T_s\right\| < 843Nm)$ $9.8 \times 10^5 (\left\|T_s\right\| \ge 843Nm)$

6. Simulation Studies

What deserved our attention is that the quadratic integral sliding mode control could be applied to the uncertain systems with linear time-invariant nominal plants, where $f(x,t) = Ax$, $g(x,t) = B$, A is the system matrix, and B is the input matrix.

The harmonic gear drive system parameters [6], which are shown in Table 1, are used in following simulations. Substituting parameters into harmonic gear drive systems model (13), then the system will be

$$\begin{cases} \dot{x}_1 = x_2 \\ \dot{x}_2 = -9.897 \times 10^6 x_1 - 69.9855 x_2 + 7.918 \times 10^8 x_3 + 148.188 u(t) \\ \dot{x}_3 = x_4 \\ \dot{x}_4 = 2.8723 \times 10^5 x_1 - 2.297 \times 10^7 x_3 \end{cases} + \Delta A x + \Delta B u(t) + T_u(x) \tag{49}$$

$$\Delta A x = \begin{bmatrix} 0.1 x_2 \\ -9.897 \times 10^5 x_1 - 6.99855 x_2 + 7.918 \times 10^7 x_3 \\ 0.1 x_4 \\ 2.8723 \times 10^4 x_1 - 2.297 \times 10^6 x_3 \end{bmatrix},$$

$$T_u(x) = \begin{bmatrix} 0 \\ T_m(x) - T_{ul}(x) \\ 0 \\ T_l(x) + T_{ul}(x) \end{bmatrix}, \tag{50}$$

$$\Delta B = \begin{bmatrix} 0 \\ 7.4094 \\ 0 \\ 0 \end{bmatrix},$$

$$T_m(x) = \frac{1}{6.82 \times 10^{-4}} \begin{cases} -\psi_m, & \dot{x}_1 = 0,\ \left|\psi_m\right| \le f_{sm} \\ -\mathrm{sgn}(\psi_m) f_{sm}, & \dot{x}_1 = 0,\ \left|\psi_m\right| > f_{sm} \\ -\mathrm{sgn}(q_m) f_{cm}, & \left|\dot{x}_1\right| > 0, \end{cases}$$

$$\psi_m = -5.4 \times 10^5 \left(\frac{x_1}{80} - x_3\right) + 0.092 u(t), \tag{51}$$

$$f_{cm} = 1.5738 \times 10^{-6} {x_1}^2 - 3.7901 \times 10^{-4} x_1 + 0.0720,$$

$$f_{sm} = 1.0388 \times f_{cm}.$$

Table 2: Simulation data without uncertainties.

	Steady-state error (rad)	Maximum overshoot (rad)	Stable time (s)	Control values $\sum u_i^2\,(V^2)$	Error values $\sum e_i^2\,(rad^2)$	Maximum Control values $\max\lvert u_i\rvert\,(V)$
QISMC	0.0042	0.0472	0.0572	1.6307×10^{12}	0.1555	2.6428×10^5
ISMC	0.0024	0.0809	0.0741	2.2879×10^{12}	0.2256	4.7746×10^5
SMC	0.0070	0.0537	0.0827	1.6250×10^{12}	0.1978	2.6783×10^5

Table 3: Simulation data with uncertainties.

	Steady-state error (rad)	Maximum overshoot (rad)	Stable time (s)	Control values $\sum u_i^2(V^2)$	Error values $\sum e_i^2\,(rad^2)$	Maximum Control values $\max\lvert u_i\rvert\,(V)$
QISMC	0.0046	0.0538	0.0608	1.6206×10^{12}	0.1609	2.6428×10^5
ISMC	0.0033	0.0972	0.0846	2.2279×10^{12}	0.2408	4.7746×10^5
SMC	0.0087	0.0634	0.0901	1.6183×10^{12}	0.2192	2.6783×10^5

$$T_l(x) = \frac{1}{2.35 \times 10^{-2}} \begin{cases} -\psi_l, & \dot{x}_3 = 0,\ |\psi_l| \le f_{sl} \\ -\operatorname{sgn}(\psi_l)\, f_{sl}, & \dot{x}_3 = 0\ |\psi_l| > f_{sl} \\ -\operatorname{sgn}(q_l)\, f_{cl}, & |\dot{x}_3| > 0, \end{cases}$$

$$\psi_l = 6.75 \times 10^3 \left(\frac{x_1}{80} - x_3\right),$$

$$f_{cl} = 1.5738 \times 10^{-6} {x_3}^2 - 3.7901 \times 10^{-4} x_3 + 0.0720, \tag{52}$$

$$f_{sl} = 1.0388 \times f_{cl}.$$

$$T_{ul}(x) = 5.4 \times 10^5 \Delta e(t),$$

$$\Delta e(t) = \begin{cases} -\Delta\varphi - j, & \dfrac{x_1}{80} - x_3 - \Delta\varphi > j \\ 0, & \left|\dfrac{x_1}{80} - x_3 - \Delta\varphi\right| < j \\ -\Delta\varphi + j, & \dfrac{x_1}{80} - x_3 - \Delta\varphi < -j, \end{cases} \tag{53}$$

$$j = 0.5mm.$$

Choosing the initial state vector's condition as $x_0 = [0\ \ 0\ \ 0.05\ \ 0]$, $\sigma = 1$, $\zeta_0 = 0$, $\zeta_1 = 0$, $\lambda_0 = 60$, $\lambda_0 = 0$, $\eta_0 = 0$, and $\eta_0 = 4 + \|x\|$, suppose that the system is not affected by nonlinear mismatched uncertainties. Define the angular transmission errors as $e = q_m/r - q_l$. $u_0 = (CB)^{-1}(-CAx + \dot{\mu})$, μ is an auxiliary variable, and $\mu = Cx = [221.07\ \ 0.0833\ \ -1.515\ \ 1]\,x$, $\dot{\mu} = -5\mu$.

Simulation results in comparison with SMC and ISMC, shown in Table 2 and Figures 6–12.

As the simulation results indicated, when choosing SMC, the system has acceptable overshoot but has a larger steady state error and much longer stable time. When choosing ISMC, the system rises rapidly with a fewer steady state error but has larger control values and maximum overshoot, which will inevitably cause impact to the system.

When choosing QISMC, the system will steady rapidly with an acceptable steady state error. In comparison with SMC, control values rise a little and the relative increment is 0.2% ~ 4%. The system has minimum overshoot, minimum stable time, and minimum error values, which satisfy the requirements of high precision, fast response, and smooth operation.

Considering that the system is affected by nonlinear mismatched uncertainties, simulation results are presented in Tables 3 and 4 and Figures 13–19.

The simulation results without uncertainties (in Table 2) are compared with simulation results with uncertainties (in Table 3), and then system deterioration caused by uncertainties is demonstrated in Table 4, which will indicate system robustness against mismatched uncertainties.

As shown in results, when system is affected by uncertainties, ISMC has the most serious deterioration and simulation curves cannot keep smooth. Despite the fact that SMC can still stabilize the system, the control system quality will not be accepted after deterioration. In comparison with SMC and ISMC, QISMC can stabilized the system with a series advantages such as fast response, fewer rise time, fewer overshoot, and fewer small error. The relative control value

Table 4: System deterioration.

	Steady-state error	Maximum overshoot	Stable time	Error values
QISMC	9.52%	13.98%	6.29%	3.78%
ISMC	37.50%	20.14%	11.42%	6.8%
SMC	12.42%	13.66%	8.94%	10.8%

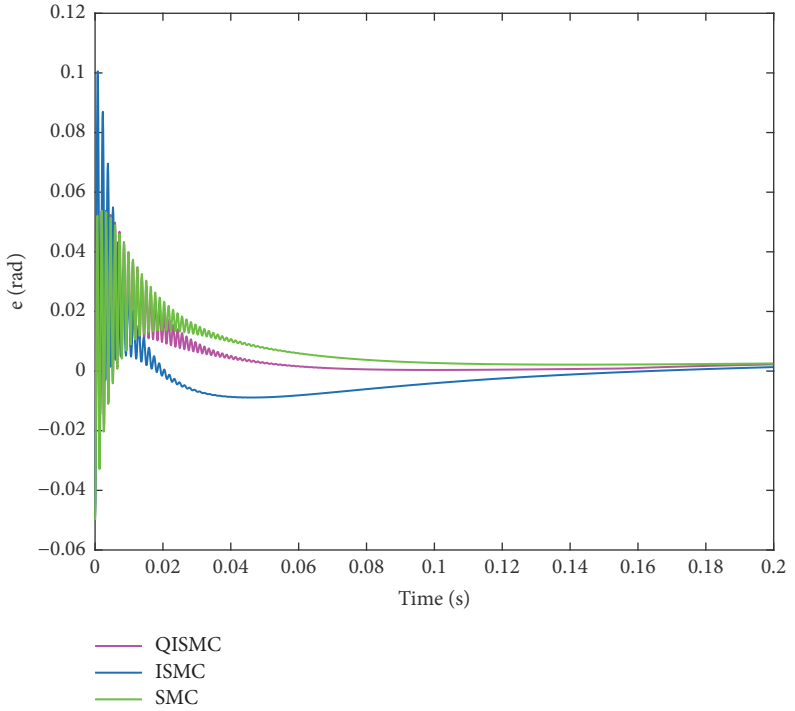

Figure 6: Angular transmission error e without uncertainties.

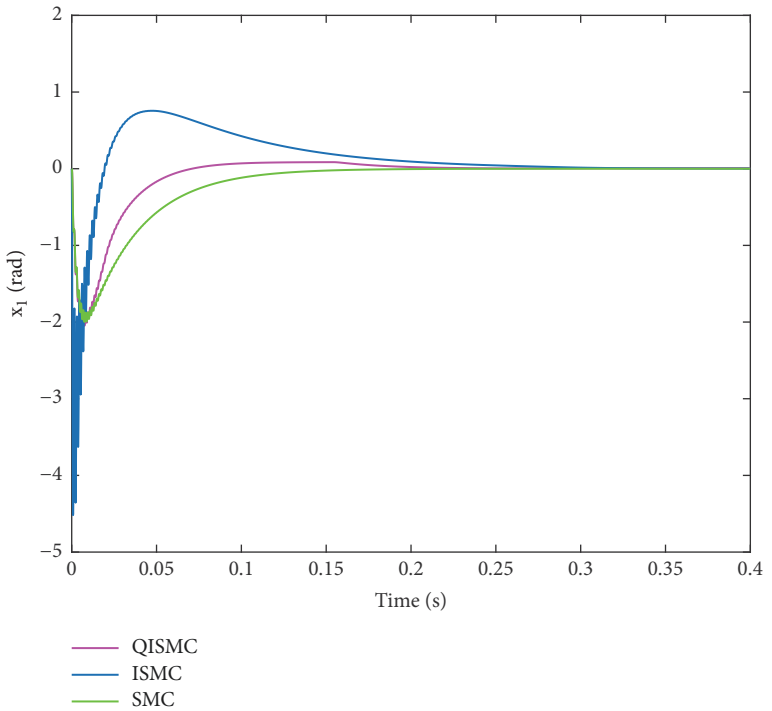

Figure 7: State vector x_1 without uncertainties.

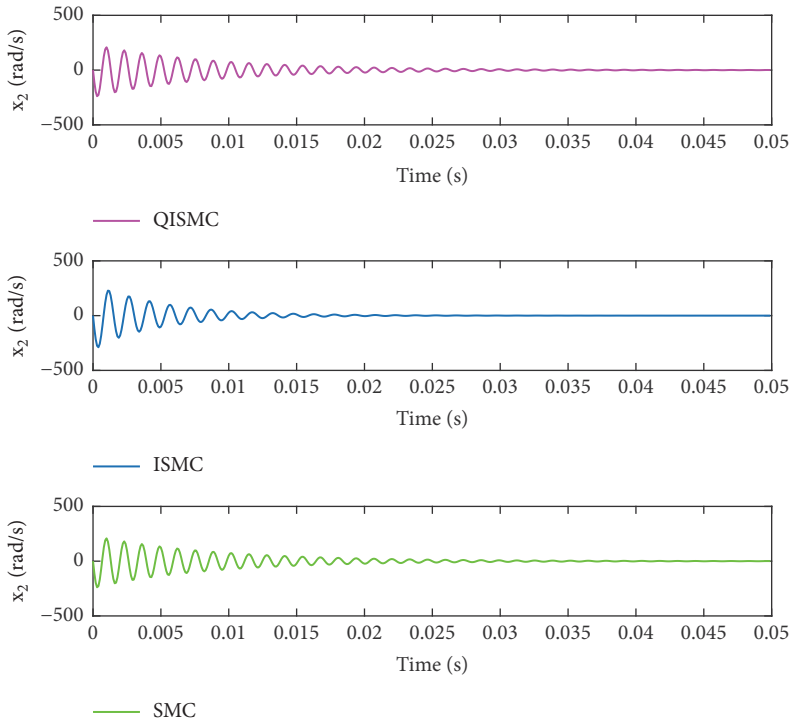

Figure 8: State vector x_2 without uncertainties.

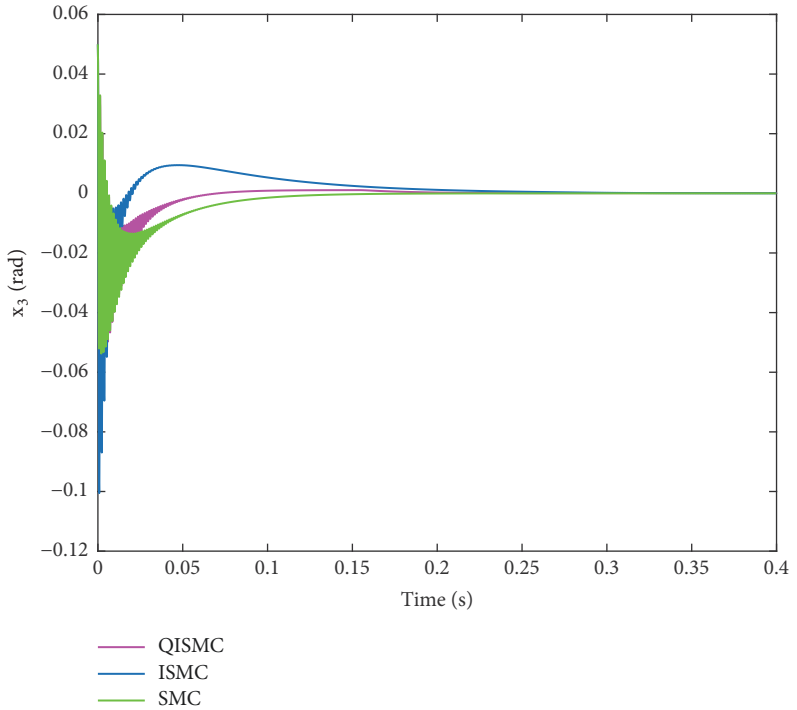

Figure 9: State vector x_3 without uncertainties.

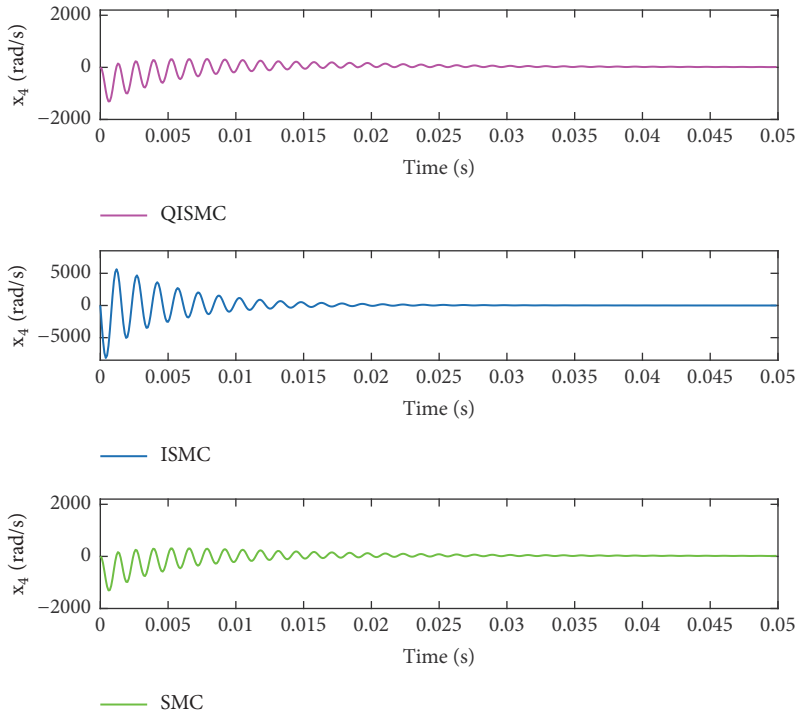

Figure 10: State vector x_4 without uncertainties.

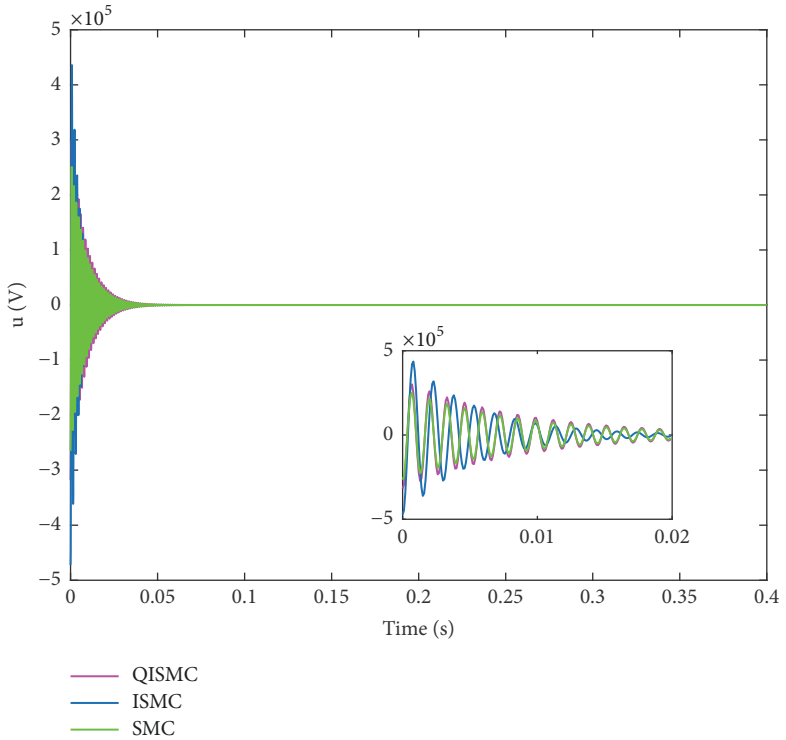

Figure 11: Control signal u without uncertainties.

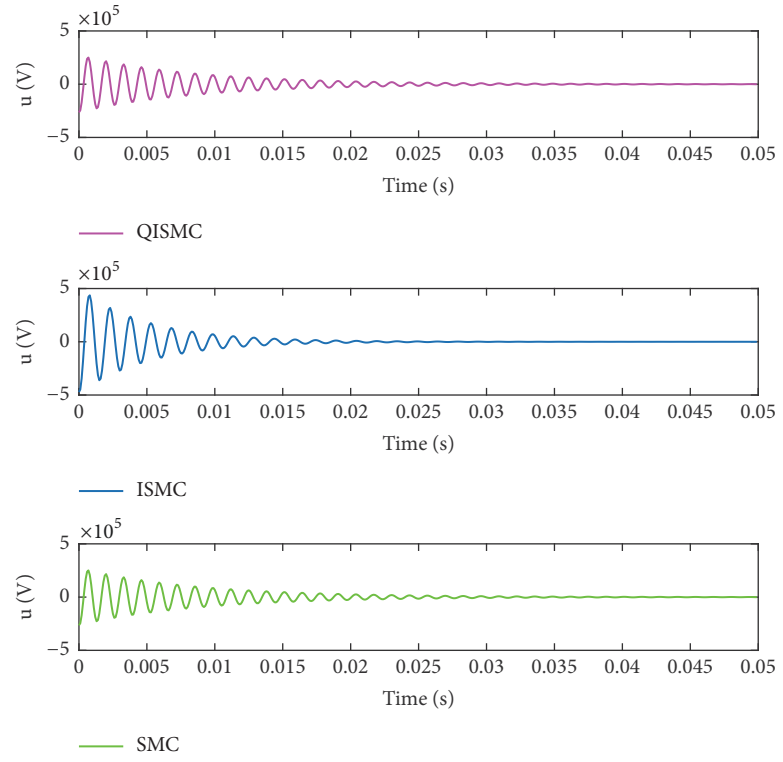

Figure 12: Comparison of control signal u without uncertainties.

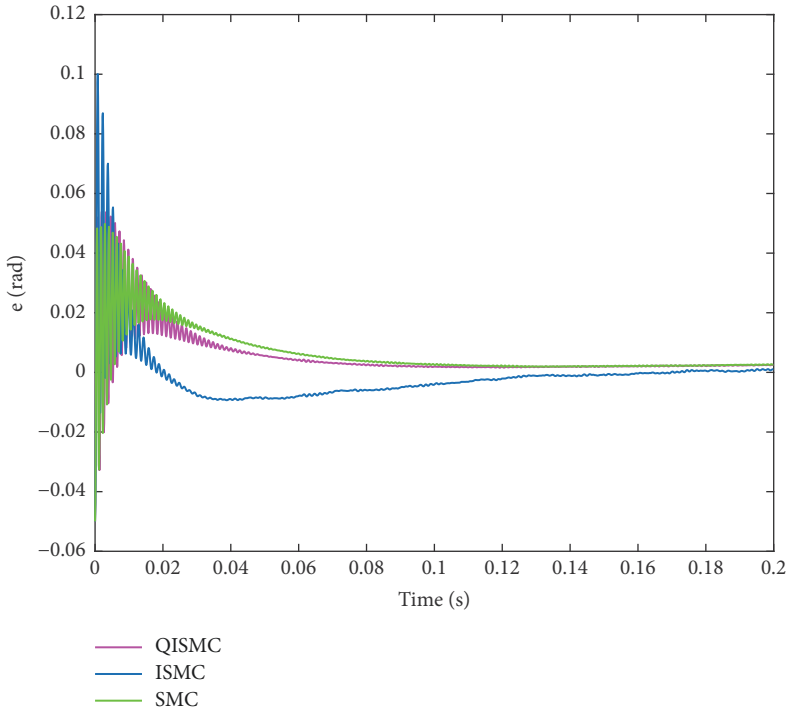

Figure 13: Angular transmission error e with uncertainties.

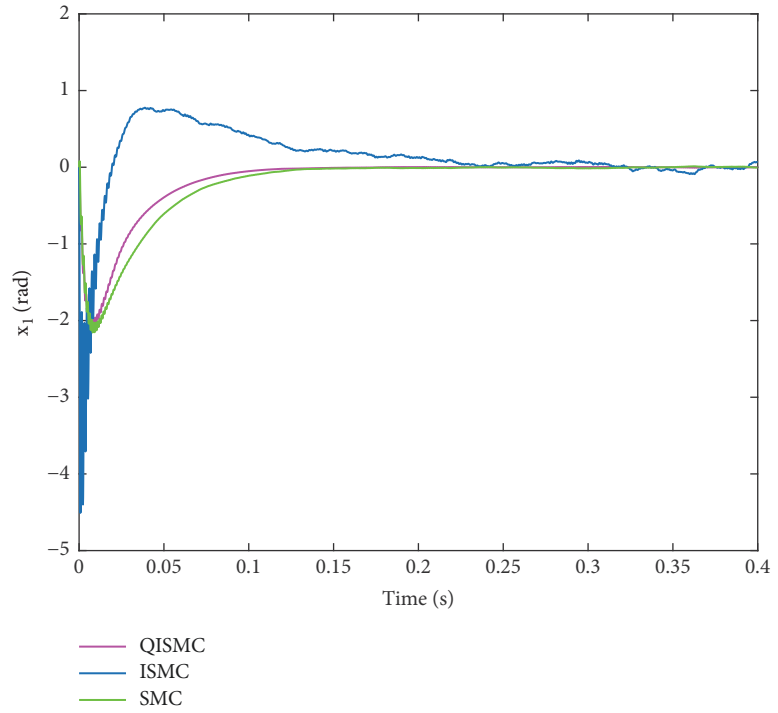

Figure 14: State vector x_1 with uncertainties.

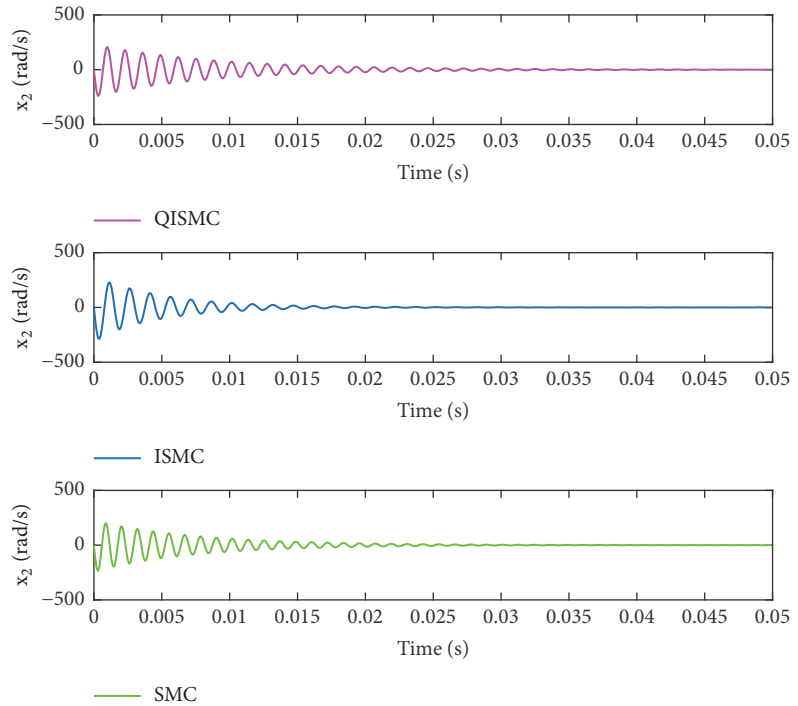

Figure 15: State vector x_2 with uncertainties.

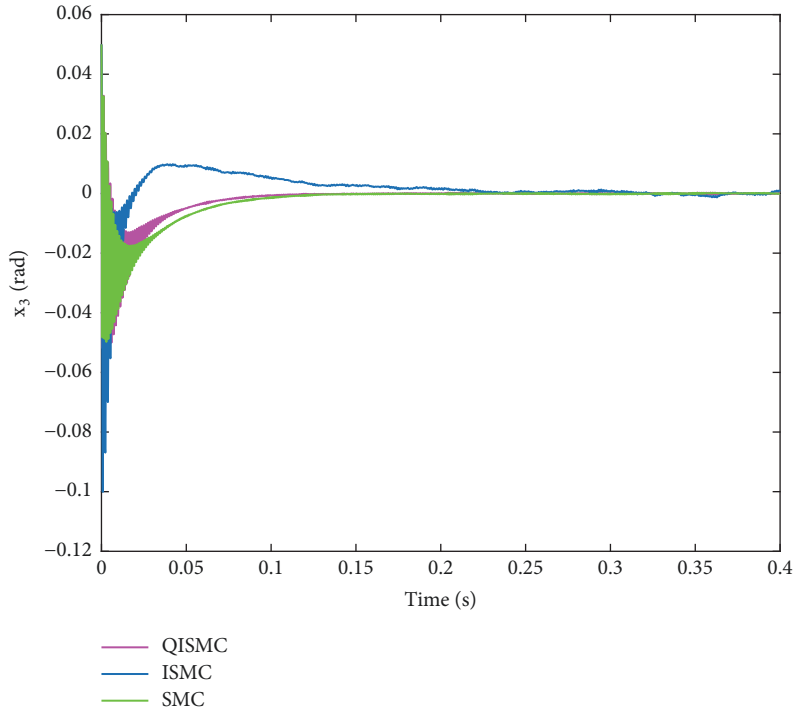

Figure 16: State vector x_3 with uncertainties.

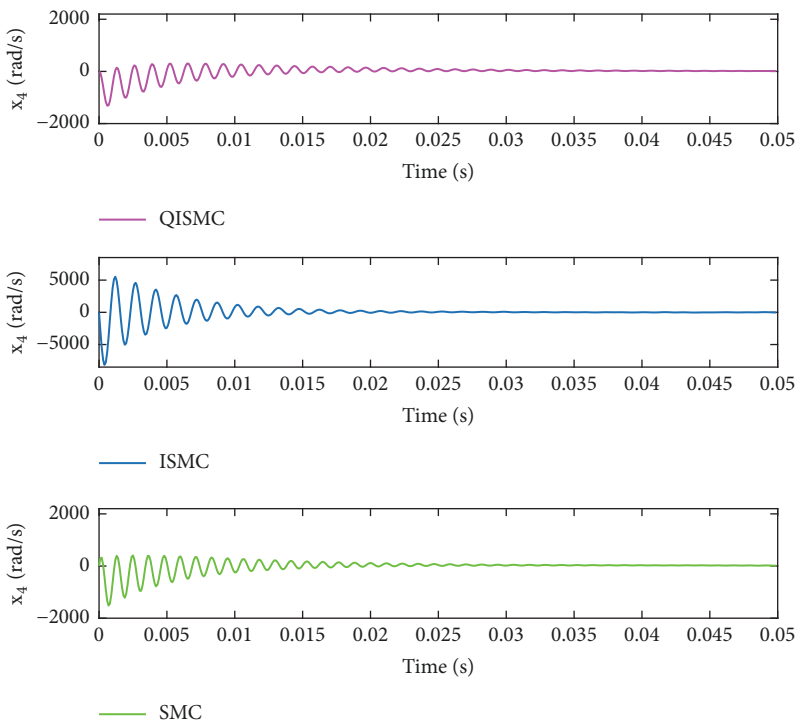

Figure 17: State vector x_4 with uncertainties.

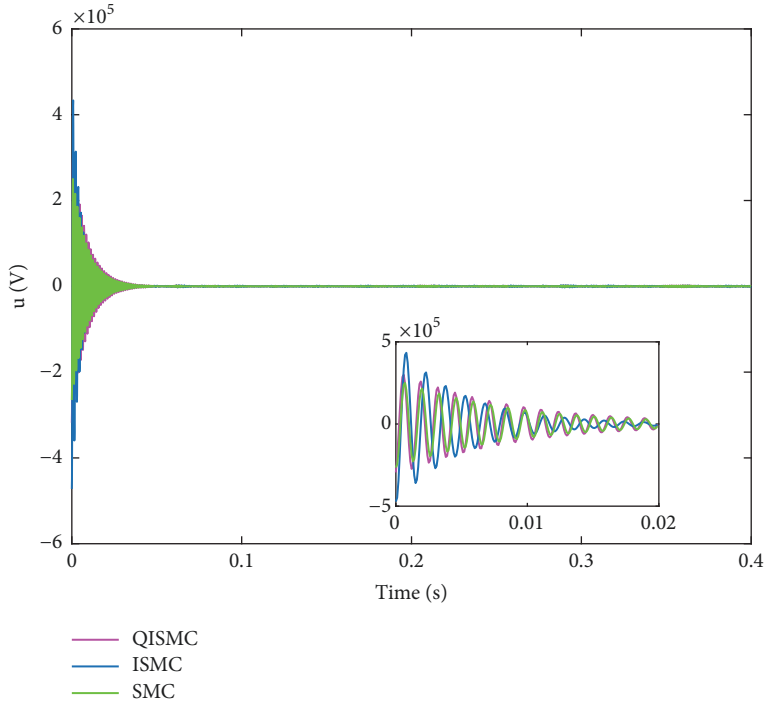

Figure 18: Control signal u with uncertainties.

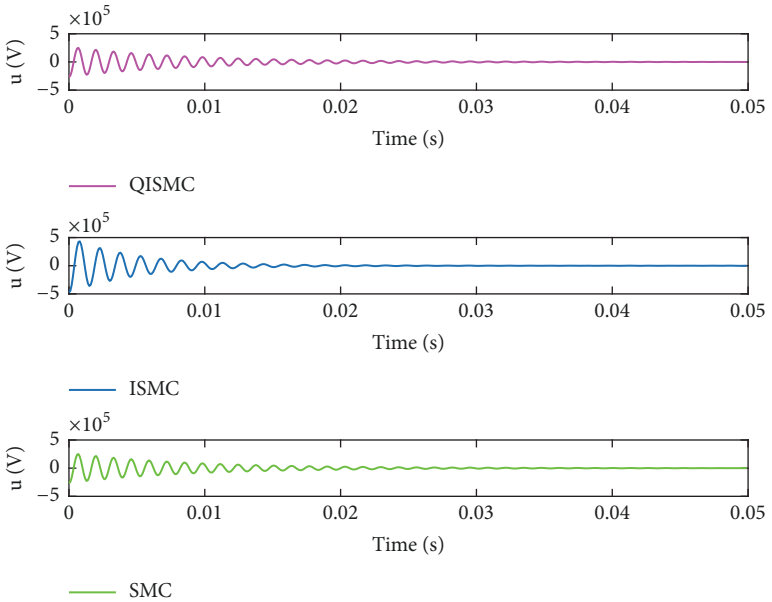

Figure 19: Comparison of control signal u with uncertainties.

increment lies in 0.2% ~ 5.3%. Simulation results illustrate that QISMC has strong robustness to nonlinear mismatched uncertainties and disturbance.

7. Conclusions

In order to compensate harmonic gear transmission errors by control method, this paper studies quadratic integral sliding mode control for a class of nonlinear harmonic gear drive systems with mismatched uncertainties, where a new quadratic integral sliding mode controller design method based on quadratic integral sliding mode surface is presented. Considering the nonlinear torques which are caused by backlash and frictions, the models of nonlinear frictions and torques are presented and the influence of nonlinear parts is compensated during control system design. In system modeling, frictions and nonlinear elastic deformations are taken into consideration and then the mathematical model of

harmonic gear drive system is established. By using Lyapunov stability theory, it is proven that the quadratic integral sliding mode can be reached in finite time and closed-loop systems are asymptotic stable robustly. Simulation studies are carried out and the results verify the effectiveness of the proposed method. Compared with the traditional linear sliding mode control (SMC) and the integral sliding mode control (ISMC), the quadratic integral sliding mode control stabilizes the system rapidly with shorter rise time, lower overshoot, smaller errors, and strong robustness against mismatched uncertainties and nonlinear disturbances. The results indicate that QISMC has a good performance with strong robustness on a class of nonlinear system with mismatched uncertainties.

Nomenclature

Notation

i_a: Motor armature current
$u(t)$: Motor armature voltage
R: Equivalent resistance
K_b: Back-EMF coefficient
ω_m: Angel speed of motor rotor
L: Motor armature inductance
q_m: Angular displacement of the wave generator
q_l: Angular displacement of the flexspline
T_m: Input torques on the wave generator
T_s: Input torque on the flexspline
F_m: Input equivalent frictions on the wave generator
F_l: Input equivalent frictions on the flexspline
J_m: Moment of inertia of the wave generator
J_l: Moment of inertia of the flexspline
r: Reduction ratio
K_s: Torsional stiffness of the harmonic gear
K_m: Motor torque coefficient
f_{cm}: Average Coulomb's frictions
f_{sm}: The static frictions
$F_m(x)$: Frictions on wave generator
$F_l(x)$: Frictions on the flexspline
j: Width of backlash
$\Delta\varphi$: Transmission error caused by nonelastic deformation torsion angle
$\Delta e(t)$: The elastic deformation torsion angle caused by backlash
$T_{ul}(x)$: Torques caused by $\Delta(t)$
ΔAx: State parameters variations
ΔB: Control signals variations.

Abbreviations

QISMC: Quadratic integral sliding mode control
ISMC: Integral sliding mode control
SMC: Sliding mode control.

Conflicts of Interest

The authors declared no potential conflicts of interest with respect to the research, authorship, and/or publication of this article.

Acknowledgments

This work is supported by the Fundamental Research Funds for the Central Universities (NS2016027) and the Nanjing University of Aeronautics and Astronautics Graduate Innovation Base (Laboratory) Open Fund (kfjj20170211, kfjj20170219).

References

[1] I. Schaefer and R. Slatter, "Precision Pointing and Actuation Systems for UAVs Using Harmonic Drive Gears," *AIAA Journal*, 2013.

[2] X. Pan, H. Wang, and Y. Jiang, "Development of a built-in torque sensor in harmonic drive gears for robots," *Chinese Journal of Scientific Instrument*, vol. 35, no. 1, pp. 154–161, 2014.

[3] Y. Ohno, N. Niguchi, and K. Hirata, "Radial Differential Magnetic Harmonic Gear," *Journal of the Japan Society of Applied Electromagnetics Mechanics*, vol. 23, no. 1, pp. 23–28, 2015.

[4] L. Dongdong, "Discussion on the micro harmonic gear transmission," in *Chinese machinery*, vol. 17, pp. 238-238, 2014.

[5] Y. Wang, W. Yang, and C. Duan, "Stress analysis of flexspline in harmonic gear reducer with composite material layer," *Modern Manufacturing Engineering*, 2014.

[6] M. Hei, S.-X. Fan, H.-B. Liao, Q.-K. Zhou, and D.-P. Fan, "Modeling of precision harmonic drive system," *Optics and precision engineering*, vol. 22, no. 7, pp. 1842–1849, 2014.

[7] T. Tjahjowidodo, F. Al-Bender, and H. van Brussel, "Theoretical modelling and experimental identification of nonlinear torsional behaviour in harmonic drives," *Mechatronics*, vol. 23, no. 5, pp. 497–504, 2013.

[8] L. Gangjun, "Mathematical model of precision harmonic drive and its control research," *Mechanical design and manufacture*, vol. 7, pp. 205–207, 2010.

[9] J. Yang, D. Liang, D. Yu, and T. Y. F. Lang, "System identification and sliding mode control design for electromechanical actuator with harmonic gear drive," in *Proceedings of the 28th Chinese Control and Decision Conference, CCDC 2016*, pp. 5641–5645, China, May 2016.

[10] X. Jian, "Study on optimal design of hydraulic pump-control-motor system speed sliding mode control," *Computer Simulation*, vol. 33, no. 5, 2016.

[11] N. E. Sadr and H. R. Momeni, "Fuzzy Sliding mode Control for missile autopilot design," in *Proceedings of the 2011 IEEE GCC Conference and Exhibition*, pp. 453–456, UAE, February 2011.

[12] M. Furat and I. Eker, "Second-order integral sliding-mode control with experimental application," *ISA Transactions*, vol. 53, no. 5, pp. 1661–1669, 2014.

[13] A. T. Azar and F. E. Serrano, "Adaptive Sliding Mode Control of the Furuta Pendulum," in *Advances and Applications in Sliding Mode Control systems*, pp. 1–42, Springer, 2015.

[14] D. Ginoya, P. D. Shendge, and S. B. Phadke, "Sliding mode control for mismatched uncertain systems using an extended disturbance observer," *IEEE Transactions on Industrial Electronics*, vol. 61, no. 4, pp. 1983–1992, 2014.

[15] R. A. Hess and M. Bakhtiari-Nejad, "Sliding-mode control of a nonlinear model of an unmanned aerial vehicle," *Journal of Guidance, Control, and Dynamics*, vol. 31, no. 4, pp. 1163–1166, 2008.

[16] Li. Gangjun, "A mathematical model of harmonic gear used for precise position control," in *Mechanical Transmission*, vol. 34, pp. 26–29, 2010.

[17] J. Yang H and C. Fu L, "Nonlinear adaptive control for manipulator system with gear backlash," in *Proceedings of 35th IEEE Conference on Decision and Control*, vol. 4, pp. 4369–4374, IEEE, 1996.

[18] M. L. Corradini and G. Orlando, "Robust stabilization of nonlinear uncertain plants with backlash or dead zone in the actuator," *IEEE Transactions on Control Systems Technology*, vol. 10, no. 1, pp. 158–166, 2002.